Available online at www.sciencedirect.com
ScienceDirect
Journal of Colloid and Interface Science 308 (2007) 491–499
JOURNAL OF Colloid and Interface Science
www.elsevier.com/locate/jcis

Formation of nanoparticles in water-in-oil microemulsions controlled by the yield of hydrated electron: The controlled reduction of Cu^{2+}

Qingde Chen, Xinghai Shen *, Hongcheng Gao

Beijing National Laboratory for Molecular Sciences, Department of Applied Chemistry, College of Chemistry and Molecular Engineering, Peking University, Beijing 100871, People's Republic of China

Received 13 August 2006; accepted 7 December 2006

Available online 6 February 2007

Abstract

In the water-in-oil (W/O) microemulsions based on nonionic surfactants, i.e., Brij 30, Brij 56, or Triton X-100, the ω value (molar ratio of water to surfactant), anion, and surfactant could remarkably affect the radiolytic reduction of Cu^{2+} and the morphologies of the reduction products simultaneously. The addition of toluene or naphthalene could transform the reduction products from copper to cuprous oxide in the Brij 56-based microemulsion, and the efficiency of naphthalene was obviously higher than that of toluene. After the effects of pH value and cosurfactant were excluded, it could be concluded that the effects of the ω value, the anion, and the structure of the surfactant on the yield of hydrated electrons (e^-_{aq}) play a key role in the radiolytic reduction of Cu^{2+}. It was also suggested that the morphology of the reduction product may be controlled by the yield of e^-_{aq}.

Keywords: Microemulsion; Hydrated electrons; γ-Irradiation; Cuprous oxide; Copper nanoparticles; Controlled reduction

1. Introduction

Synthesis of inorganic nanoparticles still remains challenging due to difficulties in the control of the composition and morphology [1–4]. To overcome this problem, a clear picture of the mechanism will be helpful. Among the numerous synthetic methods, water-in-oil (W/O) microemulsions or reversed micelles can provide us with a particularly attractive microreactor for preparing nanoparticles, where the morphology of nanoparticles can be well controlled [1,5–9]. Generally, surfactant, cosurfactant, anion, and ω value (molar ratio of water to surfactant) can only affect the shape of nanoparticles synthesized by routine chemical methods via their effect on the structure of the microemulsion (the rigidity of the interface, the size of the water pool, etc.) or via the adsorption action of the surfactant on the surface of the nanoparticles [1,7–12].

Differently from routine chemical reactions, γ-irradiation is another powerful method of preparing nanoparticles [13,14]. And the combination of γ-irradiation and W/O microemulsion has become a novel and important method in the synthesis of nanoparticles. So far, Ag [15–18], Cd [19], Pd [19], Cu [19], CdS [20], ZnS [20], and PbS [21] nanoparticles have been synthesized by this means. Very recently, our research group has successfully synthesized Ag nanoparticles [22] and Cu_2O octahedron nanocrystals [23] by this method. Moreover, their growth process was traced by absorption [23] or photoluminescence [22] spectra, respectively. However, in the course of research, we found something bewildering. In Triton X-100-based microemulsions, we got Cu_2O octahedron nanocrystals from $Cu(NO_3)_2$ by γ-irradiation [23]. In the same system, Qi et al. [24] synthesized Cu nanoparticles from $CuCl_2$ by routine chemical reduction. In addition, in sodium dodecyl sulfate (SDS)-based microemulsion, a complex of Cu^+ with SDS was obtained from $CuSO_4$ by γ-irradiation [19]. It is evident that different copper sources and different surfactants, as well as different methods (γ-irradiation method or chemical method), can result in different reduction products. This encourages us to systematically explore the regularity of the radiolytic reduction of Cu^{2+} in microemulsion and clarify the mechanism, which will favor the morphology control of Cu and Cu_2O nanoparti-

* Corresponding author. Fax: +86 10 62759191.
E-mail address: xshen@pku.edu.cn (X. Shen).

0021-9797/$ – see front matter
doi:10.1016/j.jcis.2006.12.021

cles with great freedom and will be helpful for the synthesis of other nanoparticles in microemulsion.

According to the results of pulse radiolytic investigation of the microemulsion system, when a microemulsion is irradiated, hydrated electrons (e_{aq}^-) can be generated mainly from the scavenging of excess electrons, which are produced originally through the radiolysis of oil, by the water pool [25–28]. In addition, the radiolysis of water in the water pool can also generate e_{aq}^- directly, but it is less important [25–28]. As the ω value increases, the yield of e_{aq}^- usually increases, except in the cationic-surfactant-based microemulsions [25–30]. In the SDS-based microemulsion, Kapoor et al. [16,19] have used this regularity to explain the radiolytic synthesis of Ag, Cd, Pd, and Cu nanoparticles. In the same microemulsion, they also studied the reduction of Tl^+, Co^{2+}, and Ni^{2+} by pulse radiolysis and found that the rate constants for the reduction of these cations by e_{aq}^- were much lower than those in aqueous solution [17].

In this paper, a more systematic work will be reported, in which we explore how the ω value, the anion (the counterion of Cu^{2+}), and the structure of the surfactant affect the radiolytic reduction of Cu^{2+} in nonionic-surfactant-based microemulsions. Our results demonstrate that their effects on the yield of e_{aq}^- play a key role. It is also suggested that the morphology of nanoparticles may be controlled by the yield of e_{aq}^-. Here, it should be pointed out that the above results are remarkably different from the mechanism of ω value, anion, and surfactant only affecting the morphology of nanoparticles synthesized by routine chemical methods, as mentioned above. It should also be noted that the present work further confirms the validation of the mechanism for the producing of hydrated electrons in W/O microemulsions, which is quite important in radiation chemistry.

2. Materials and methods

2.1. Chemicals

Brij 30 ($CH_3(CH_2)_{10}CH_2(OCH_2CH_2)_4OH$, Acros), Brij 56 ($CH_3(CH_2)_{14}CH_2(OCH_2CH_2)_{10}OH$, Aldrich), Triton X-100 ($(CH_3)_3CCH_2C(CH_3)_2C_6H_4(OCH_2CH_2)_{10}OH$, CP, Beijing Chemical Reagents Inc.), cyclohexane (AR, Beijing Chemical Reagents Inc.), copper sulfate, copper chloride, toluene, naphthalene, nitric acid (AR, Beijing Chemical Plant), *n*-hexanol, copper nitrate (AR, Beijing Yili Fine Chemical Products Inc.), copper bromide (AR, Shanghai Zhenxin Reagent Plant), and dodecyl mercaptan (CP, Nankai Fine Chemical Plant) were used as received. Deionized and tridistilled water was used in the experiments.

2.2. Synthesis of nanoparticles

A certain amount of copper salt was dissolved in water to obtain a 0.02 mol/L stock solution. To prepare microemulsions, surfactant (Triton X-100 or Brij 56), *n*-hexanol, and cyclohexane with the molar ratio 1.0:1.6:57.6 were first mixed and then a certain volume of the above stock solution was added, with the ω value fixed at 9.0. The mixtures were stirred at room temperature until they became transparent. In the Brij 30-based microemulsions, the cosurfactant was not used and the ω value was fixed at 7.0 except as stated otherwise. After being bubbled with high-purity N_2 under anaerobic conditions, the microemulsions were irradiated in a field of a ^{60}Co γ-ray source for 16 h and 40 min with an absorbed dosage of 40 kGy.

2.3. Characterization

After irradiation, the absorption spectra were recorded immediately on a U-3010 spectrometer with the identical systems without being irradiated as standard. If the absorption spectra did not change with time, the corresponding samples were deemulsified, washed by ethanol, and then dispersed in ethanol by ultrasonication. In the case of the absorption spectra changing with time, plenty of dodecyl mercaptan was added into the microemulsions. After 48 h, the precipitate was collected by centrifugation, rinsed with ethanol, and dispersed in chloroform by ultrasonication. The obtained dispersion was dropped onto a carbon-coated copper grid. After the solvent was evaporated at room temperature, the transmission electron microscopy (TEM) and the selected area electron diffraction (SAED) images were conducted on a JEOL JEM-200CX microscope operated at 160 kV. The range of the nanoparticles' size was determined after measuring the dimensions of more than 500 nanoparticles in sight of the obtained micrograph. After the dispersed sample was deposited on a piece of glass, powder X-ray diffraction (XRD) pattern was recorded on a Rigaku Dmax-2000 diffractometer with Cu$K\alpha$ radiation ($\lambda = 0.15418$ nm) and X-ray photoelectron spectrum (XPS) was collected on a Kratos Axis Ultra spectrometer with monochromatized Al$K\alpha$ radiation.

3. Results

In the experiments, we found that the ω value, surfactant, and anion in W/O microemulsions could remarkably affect the radiolytic reduction of Cu^{2+} and that the morphologies of the reduction products could also be changed simultaneously. Moreover, the effects of aromatic ring, pH value, and cosurfactant were also investigated.

3.1. Effect of the ω value

In the Brij 30-based microemulsion with $Cu(NO_3)_2$ as precursor, the absorption spectra of the reduction products are clearly different when the ω value increases (Fig. 1A). With an ω value of 4.5, the absorption spectrum of the reduction product exhibits characteristic excitonic structures of semiconductor at ca. 450 nm, suggesting the generation of Cu_2O [31]. With a higher ω value of 7.0, an absorption peak at ca. 570 nm, corresponding to the surface plasma (SP) absorption of Cu nanoparticles [8,32], was observed, which indicates the formation of Cu nanoparticles. Adjusting the ω value to 5.4 between the above two values, a peak at ca. 570 nm and a shoulder peak at ca. 450 nm were observed, implying the generation of Cu and Cu_2O simultaneously.

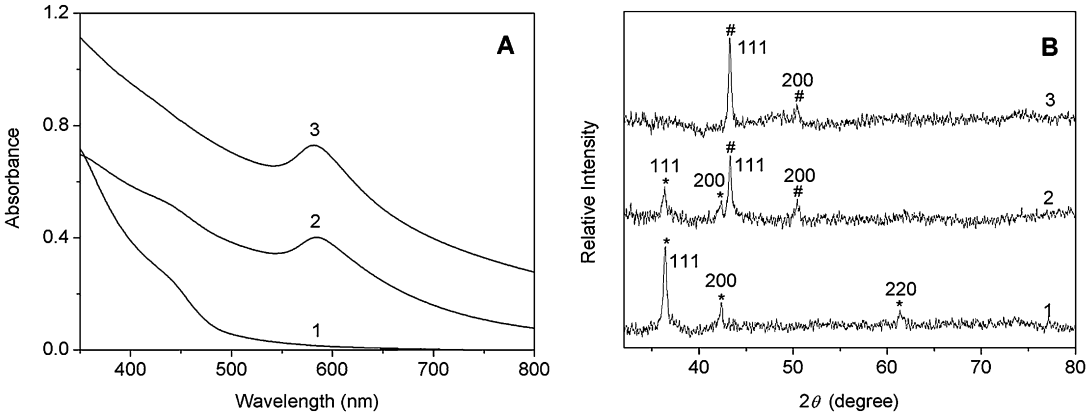

Fig. 1. Absorption spectra (A) and XRD patterns (B) of the reduction products of $Cu(NO_3)_2$ in the Brij 30-based microemulsions by γ-irradiation at different ω values (from 1 to 3, $\omega = 4.5, 5.4, 7.0$). * represents Cu_2O; # represents Cu. Before irradiation, the compositions of the microemulsion are $n_{Brij30} = 2.47$ mmol, $n_{cyclohexane} = 0.142$ mol. In the water pool, $[Cu^{2+}] = 0.02$ mol/L.

Fig. 1B shows the XRD patterns of the reduction products. With an ω value of 4.5, the interplanar distances calculated for (111), (200), and (220) from the XRD pattern match well with the standard data of cubic phase Cu_2O (JCPDS file No. 05-0667), confirming the formation of cubic phase Cu_2O. This has been further confirmed from the corresponding SAED analysis (inset, Fig. 2A), in which the observed six fringe patterns with plane distances of 0.301, 0.246, 0.213, 0.174, 0.151, and 0.128 nm are consistent with the cubic phase Cu_2O (110), (111), (200), (211), (220), and (311) plane distances of 0.3020, 0.2465, 0.2135, 0.1743, 0.1510, and 0.1287 nm. At a higher ω value of 7.0, the interplanar distances calculated for (111) and (200) from the XRD pattern (Fig. 1B) match well with the standard data of fcc metal Cu (JCPDS file No. 04-0836), demonstrating the formation of Cu particles. The corresponding SAED image (inset, Fig. 2C) reveals that the observed four fringe patterns with plane distances of 0.209, 0.180, 0.127, and 0.109 nm are consistent with the fcc metal Cu (111), (200), (220), and (311) with the corresponding plane distances of 0.2088, 0.1808, 0.1273, and 0.1090 nm, respectively, which further confirms the generation of Cu particles. When the ω value is 5.4, four apparent diffraction peaks appear in its XRD spectrum (Fig. 1B), which correspond to the (111), (200) diffraction peaks of cubic phase Cu_2O and fcc metal Cu, respectively, displaying the generation of both Cu and Cu_2O. This is further confirmed by the corresponding SAED analysis (inset, Fig. 2B), which shows the (111), (200), (220), (311) diffraction rings of the fcc metal Cu and the (110), (111), (220) diffraction rings of the cubic phase Cu_2O.

At the ω value of 4.5, the reduction product is composed of aggregated quasi-spherical nanoparticles, whose diameter is about 10 nm (Fig. 2A). At the ω value of 5.4, the reduction products are composed of rodlike, square-shaped, triangular, and quasi-spherical nanoparticles (Fig. 2B). Contrasting Fig. 2C and the supporting information (SI-1), it can be found that the aspect ratio of the rodlike nanoparticles increases with increasing ω value from 6.0 to 7.0, while the reduction products are still Cu nanoparticles. Thus, it can be concluded that the reduction product of $Cu(NO_3)_2$ can be transformed from Cu_2O to Cu when the ω value increases.

3.2. Effect of anion

In the Triton X-100-based microemulsions, where the ω value is fixed at 9.0, the absorption spectra of the reduction products of different precursors by γ-irradiation are shown in Fig. 3A. When $Cu(NO_3)_2$ is used as precursor, a shoulder peak with characteristic semiconductor excitonic structures appears around 450 nm in the absorption spectrum, indicating the generation of Cu_2O according to the discussion above. This is confirmed by the corresponding SAED (inset, Fig. $4A_1$) and XRD (curve a in Fig. 5) measurements. As illustrated by the TEM picture in Fig. $4A_1$, the projective images of these nanoparticles are almost quadrilateral, with smooth edges of 65 ± 5 nm length, and the equatorial part is darker than the polar part. According to our previous results [23], these nanoparticles are octahedral. When $CuSO_4$ is used as precursor, a broad absorption peak at ca. 470 nm suggests the formation of Cu_2O according to its characteristic absorption [23,33]. This is further verified by the corresponding SAED (inset, Fig. $4A_2$) analysis. From the corresponding TEM picture shown in Fig. $4A_2$, it can be clearly seen that the projective images of these nanoparticles are almost square, with coarse edges of 160 ± 20 nm length. The occurrence of coarse surface of these nanoparticles may be attributed to the effect of anion on the shape of nanoparticles [34]. When $CuCl_2$ and $CuBr_2$ are used as precursors, the peak at ca. 570 nm appears in their absorption spectra (curves c and d in Fig. 3A) corresponding to the SP absorption of Cu nanoparticles. This is verified by the XRD patterns of the reduction product of $CuCl_2$ (curve b in Fig. 5). The corresponding TEM images (Figs. $4A_3$ and $4A_4$) show that these reduction products are almost composed of monodispersed spherical nanoparticles, with diameter of about 5 and 5–10 nm, respectively. Especially, the Cu nanoparticles obtained from $CuCl_2$ tend to form a superlattice structure.

In the Brij 56-based microemulsions with the ω value fixed at 9.0, the absorption spectra of the reduction products of different precursors by γ-irradiation are shown in Fig. 3B. When $CuSO_4$, $CuCl_2$, and $CuBr_2$ are used as precursors, respectively, it can be seen that there appears SP absorption of Cu nanoparticles at ca. 570 nm, indicating that Cu nanoparticles are formed.

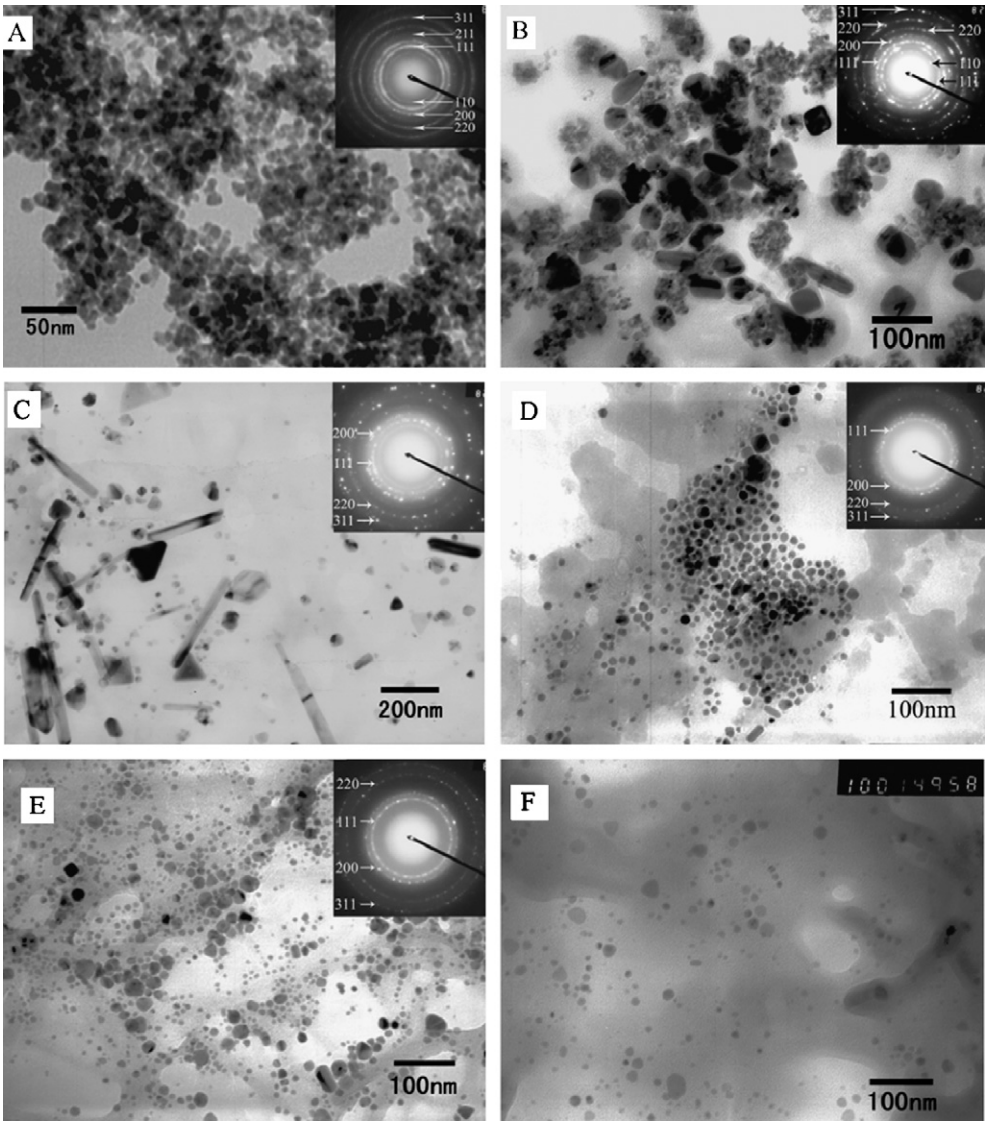

Fig. 2. Morphologies of the reduction products of Cu^{2+} in the Brij 30-based microemulsions by γ-irradiation at different ω values (from A to F, $\omega = 4.5$, 5.4, 7.0, 7.0, 7.0, 7.0) and in the presence of different precursors: (A–C) $Cu(NO_3)_2$, (D) $CuSO_4$, (E) $CuCl_2$, (F) $CuBr_2$. The insets show the SAED patterns of the corresponding products.

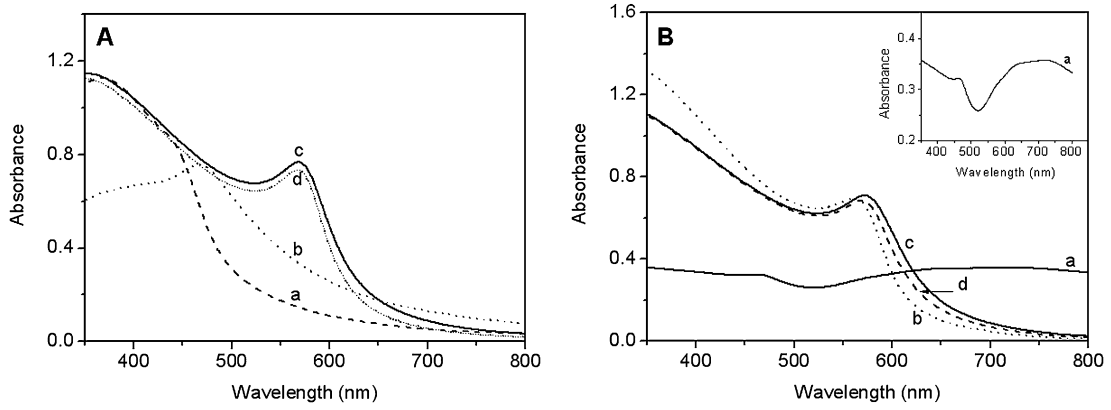

Fig. 3. Absorption spectra of the reduction products of Cu^{2+} in the Triton X-100-based (A) and Brij 56-based (B) microemulsions ($\omega = 9.0$) by γ-irradiation in the presence of different precursors: (a) $Cu(NO_3)_2$, (b) $CuSO_4$, (c) $CuCl_2$, (d) $CuBr_2$. The inset shows the enlargement of curve a in part B. Before irradiation, the compositions of the microemulsion are $n_{\text{Triton X-100}}$ (or n_{Brij56}) = 2.47 mmol, $n_{n\text{-hexanol}} = 3.95$ mmol, $n_{\text{cyclohexane}} = 0.142$ mol. In the water pool, $[Cu^{2+}] = 0.02$ mol/L.

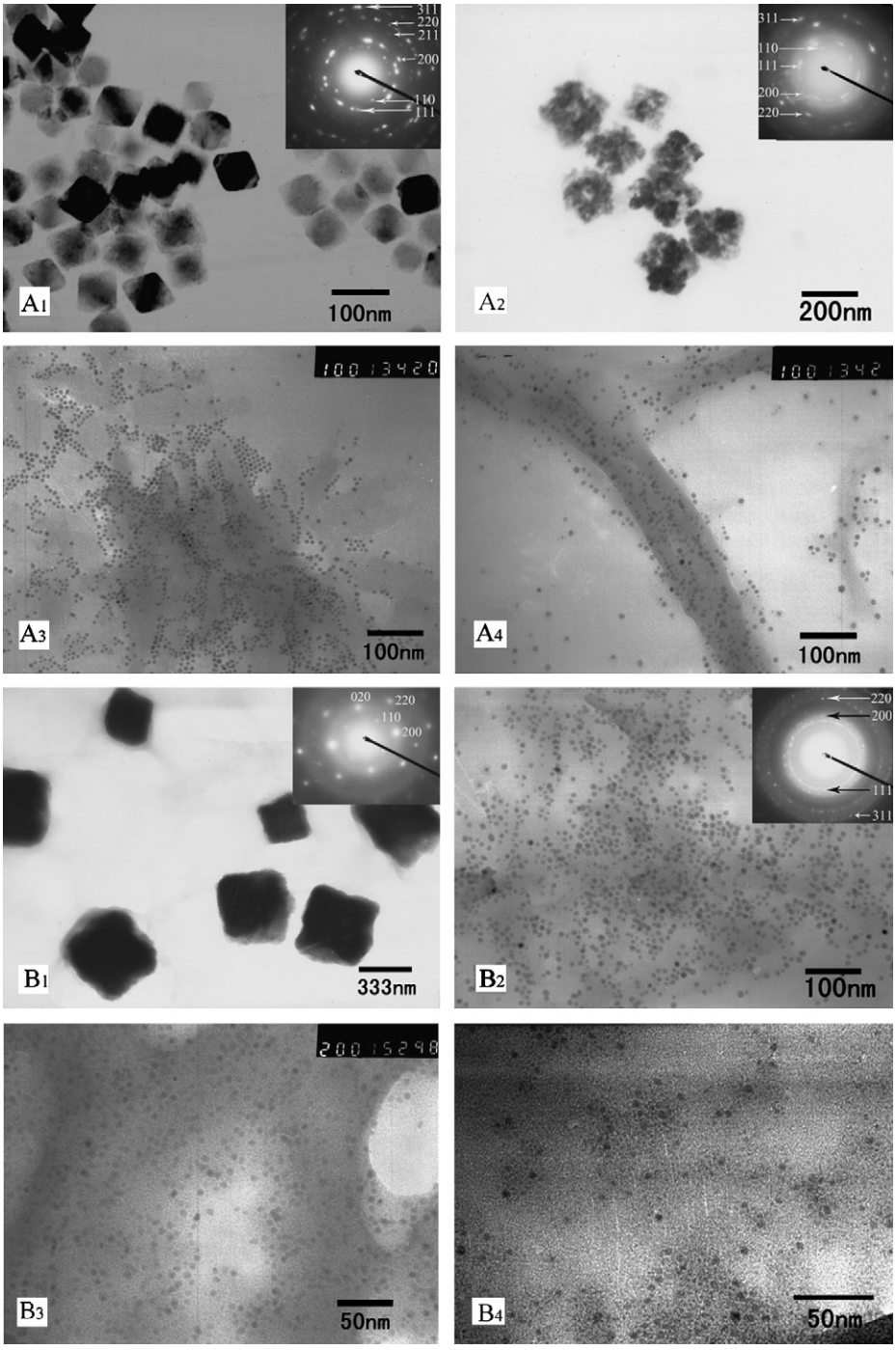

Fig. 4. Morphologies of the reduction products of Cu^{2+} in the Triton X-100-based (A) and Brij 56-based (B) microemulsions ($\omega = 9.0$) by γ-irradiation in the presence of different precursors: $Cu(NO_3)_2$ (A_1, B_1), $CuSO_4$ (A_2, B_2), $CuCl_2$ (A_3, B_3), $CuBr_2$ (A_4, B_4). The insets show the SAED patterns of the corresponding products.

In the case of $CuSO_4$ as precursor, the formation of Cu nanoparticles is substantiated by the SAED analysis (inset, Fig. $4B_2$). The corresponding TEM images for three cases (Figs. $4B_2$–$4B_4$) show that these reduction products are all composed of monodispersed spherical nanoparticles, with the diameters of 4–10, 4–6, and 3–6 nm, respectively. When $Cu(NO_3)_2$ is used as precursor, there exist a shoulder peak at ca. 450 nm and a broad absorption peak at ca. 700 nm in the absorption spectrum (curve a in Fig. 3B), implying the generation of Cu_2O according to the results in the literature [35]. This is approved by the corresponding SAED analysis (inset, Fig. $4B_1$), which indicates a highly preferred (001) orientation texture structure. The further evidence comes from the XPS analysis, which presents a binding energy of 932.32 eV for Cu $2p_{3/2}$, close to the value in the literature [36,37]. The broad absorption peak at ca. 700 nm (curve a in Fig. 3B) may be ascribed to the presence of some surface states of Cu_2O nanoparticles within the band gap [35]. The corresponding TEM images (Fig. $4B_1$) show that the reduc-

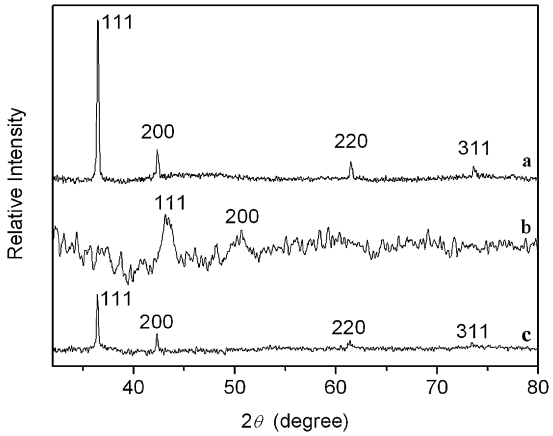

Fig. 5. XRD patterns of the reduction products of Cu^{2+} in the Triton X-100-based (a and b) and Brij 56-based (c, [toluene] = 1.86 mol/L) microemulsions ($\omega = 9.0$) by γ-irradiation in the presence of different precursors: (a) $Cu(NO_3)_2$, (b) $CuCl_2$, (c) $CuSO_4$.

Table 1
Summary of the reduction products of Cu^{2+} under different conditions

Surfactant	ω	$Cu(NO_3)_2$	$CuSO_4$	$CuCl_2$	$CuBr_2$
Triton X-100	9.0	Cu_2O	Cu_2O	Cu	Cu
	12.0	Cu_2O	–	–	–
Brij 56	9.0	Cu_2O	Cu	Cu	Cu
Brij 30	4.5	Cu_2O	–	–	–
	5.4	Cu_2O & Cu	–	–	–
	6.0	Cu	–	–	–
	7.0	Cu	Cu	Cu	Cu

tion products are mostly composed of square-shaped nanoparticles with edge length ranging from 300 to 550 nm.

In the Brij 30-based microemulsions, where the ω value is fixed at 7.0, the absorption spectra (Fig. 1A and SI-2 in supporting information) and SAED analysis (insets, Figs. 2C–2E) show that the reduction products of $Cu(NO_3)_2$, $CuSO_4$, $CuCl_2$, and $CuBr_2$ are all Cu. The corresponding TEM images indicate that the reduction products of $CuSO_4$, $CuCl_2$, and $CuBr_2$ are all composed of quasi-spherical nanoparticles besides a few rodlike nanoparticles (Figs. 2D–2F), while that of $Cu(NO_3)_2$ is composed of rodlike, square-shaped, triangular, and quasi-spherical nanoparticles (Fig. 2C).

According to the above results, it can be seen that the ω value, surfactant, and anion could remarkably affect the radiolytic reduction of Cu^{2+}. All these results are summarized in Table 1. Moreover, it can be found that the morphology of the reduction products could also be changed simultaneously.

3.3. Effect of aromatic ring

In the Triton X-100 and Brij 56 systems, it is strange that the reduction products of $CuSO_4$ are markedly different (Table 1) although the structures of the two nonionic surfactants' hydrophilic chains are similar. Based on the molecular structures, it can be inferred that the phenyl ring in the hydrophobic chain of Triton X-100 may scavenge excess electrons in the oil

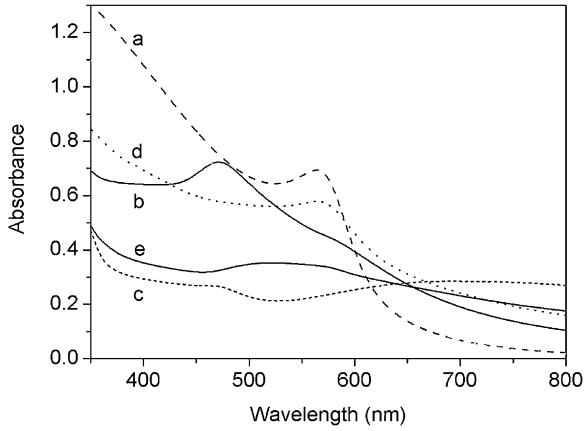

Fig. 6. Absorption spectra of the reduction products of $CuSO_4$ in the Brij-56 based microemulsions ($\omega = 9.0$) by γ-irradiation in the presence of toluene (from a to c, [toluene] = 0.56, 1.13, 1.86 mol/L, $n_{cyclohexane}$ = 0.134, 0.128, 0.107 mol) and naphthalene (from d to e, [naphthalene] = 0.16, 0.28 mol/L, $n_{cyclohexane} = 0.142$ mol). Before irradiation, the compositions of the microemulsion are $n_{Brij\ 56} = 2.47$ mmol, $n_{n\text{-hexanol}} = 3.95$ mmol. In the water pool, $[Cu^{2+}] = 0.02$ mol/L.

phase (e^-_{oil}) and H as shown in the following reactions [38–40]:

$$CH_3C_6H_5 + e^-_{oil} \xrightarrow{\text{solvent: cyclohexane}} CH_3C_6H_5^{\cdot -}, \quad k = 4.0 \times 10^9\ \text{L/(mol s)}, \tag{1}$$

$$CH_3C_6H_5 + H \rightarrow CH_3C_6H_6^{\cdot}, \quad k = 2.6 \times 10^9\ \text{L/(mol s)}. \tag{2}$$

In the present work, in order to verify the above speculation, toluene was added to the Brij 56-based microemulsion, while the total volume was not changed. Fig. 6 (curves a–c) shows the absorption spectra of the reduction products of $CuSO_4$ at different concentrations of toluene. When the concentration of toluene is 0.56 mol/L, the SP absorption of Cu nanoparticles at ca. 570 nm is observed. When the concentration of toluene is increased to 1.13 mol/L, a broad absorption peak appears around 470 nm and the SP absorption peak of Cu nanoparticles is weakened to be a shoulder peak, implying that Cu_2O has become the principal product. While the concentration of toluene is increased to 1.86 mol/L, besides a shoulder peak at ca. 470 nm, there appears a broad absorption peak at ca. 700 nm, which is similar to curve a in Fig. 3B and thus suggests the formation of Cu_2O. The TEM image (Fig. 7) shows that the reduction product is mainly composed of square-shaped nanoparticles with edge length ranging from 200 to 450 nm and their surface becomes coarse, similary to the phenomenon described in the Triton X-100 system with $CuSO_4$ as precursor. The corresponding SAED (inset, Fig. 7) and XRD (curve c in Fig. 5) analysis confirms the generation of cubic phase Cu_2O.

Naphthalene was also added into the Brij 56-based microemulsion to investigate its effect on the radiolytic reduction of $CuSO_4$. The absorption spectra of the reduction products are shown in Fig. 6 (curves d and e). It can be found that the addition of naphthalene can also transform the reduction product from Cu to Cu_2O in the microemulsion and Cu_2O has become the principal product even at the lower concentration of naph-

thalene. In other words, the efficiency of naphthalene is obviously higher than that of toluene.

3.4. Effect of pH value

Nanometer-sized Cu_2O could be obtained in aqueous systems containing SDS by the γ-irradiation method, when the pH value was carefully controlled in the range 4.0–5.0 [41]. If the pH value was in the range 3.0–3.5, Cu would appear and mix with Cu_2O [41]. However, in our previous work, Cu_2O octahedral nanocrystals were obtained without any pH adjustment of the salt solution in the Triton X-100-based W/O microemulsion by γ-irradiation [23]. We suggested that the formation mechanism of the Cu_2O nanoparticles in the microemulsion was different from that in the aqueous systems [23]. Nevertheless, no experiments have been designed to verify this speculation as yet. Here, in order to further explore the effect of pH value on the radiolytic reduction of Cu^{2+}, a control experiment was performed, in which $Cu(NO_3)_2$ was used as precursor and 0.01 mol/L HNO_3 was added to the three kinds of microemulsions. As illustrated by absorption spectra and SAED analysis of these reduction products in SI-3 (supporting information), the transformation from Cu_2O to Cu or from Cu to Cu_2O does not appear. In other words, the pH value cannot affect the radiolytic reduction of Cu^{2+} in these microemulsions. However, the morphologies of these nanoparticles are altered, which can be clearly seen in SI-3 (supporting information).

3.5. Effect of cosurfactant

The radiolytic reduction of $Cu(NO_3)_2$ in the Brij 30 system is different from those in the Triton X-100 and Brij 56 systems. Because Brij 30 can form W/O microemulsion free away from cosurfactant, *n*-hexanol, which was used as cosurfactant in the other two systems, is naturally questioned to affect the reduction of $Cu(NO_3)_2$. When *n*-hexanol was added to the Brij 30 system, the absorption spectrum and SAED analysis (SI-4, supporting information) showed that the reduction product is still Cu. Nevertheless, the aspect ratio of the rodlike Cu nanoparticles decreases (SI-4, supporting information). Thus, the above suspicion can also be excluded.

4. Discussion

The following equations [39] show the reducing reactions of Cu^{2+} by the reducing species, which are generated in the radiolysis of microemulsion, and the corresponding rate constants:

$$Cu^{2+} + e_{aq}^- \rightarrow Cu^+, \quad k = 3.3 \times 10^{10}\ \mathrm{L/(mol\,s)}, \tag{3}$$

$$Cu^{2+} + H \rightarrow Cu^+ + H^+, \quad k = 9.1 \times 10^{7}\ \mathrm{L/(mol\,s)}, \tag{4}$$

$$Cu^{+} + e_{aq}^- \rightarrow Cu, \quad k = 2.7 \times 10^{10}\ \mathrm{L/(mol\,s)}, \tag{5}$$

$$Cu^{+} + H \rightarrow CuH^+, \quad k = 5.0 \times 10^{9}\ \mathrm{L/(mol\,s)}. \tag{6}$$

It can be seen that e_{aq}^- plays an important role in the radiolytic reduction of Cu^{2+}. Moreover, the disproportionation of Cu^+ can also produce Cu atoms:

$$2Cu^+ \rightarrow Cu + Cu^{2+}. \tag{7}$$

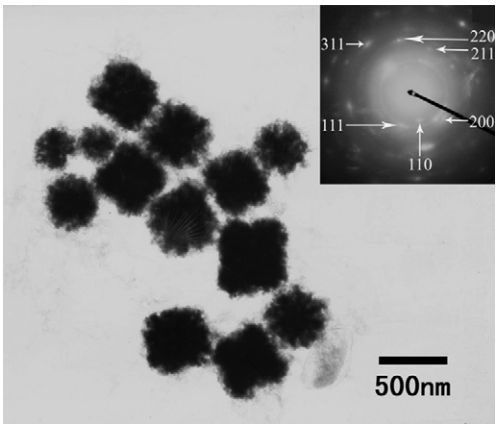

Fig. 7. Morphology of the reduction product of $CuSO_4$ in the Brij 56-based microemulsion ($\omega = 9.0$) by γ-irradiation in the presence of toluene (1.86 mol/L). The inset shows the SAED pattern.

However, a nonnegligible fact is that Cu_2O can be generated through the hydrolysis of Cu^+, which is the only source of Cu_2O:

$$Cu^+ + H_2O \rightarrow CuOH + H^+, \quad 2CuOH \rightarrow Cu_2O + H_2O. \tag{8}$$

Moreover, the addition of toluene or naphthalene can transform the reduction products from Cu to Cu_2O in the Brij 56-based microemulsion, and the efficiency of naphthalene is obviously higher than that of toluene. This indicates that electrons play a key role in the radiolytic reduction of $CuSO_4$ because the ability of naphthalene to scavenge e_{oil}^- is much stronger than that of toluene [38], while in regards of the ability to scavenge H, both of them are almost equal [39]. This is shown in Eqs. (1), (2) and the following equations:

$$C_{10}H_8 + e_{oil}^- \xrightarrow{\text{solvent: cyclohexane}} C_{10}H_8^{\bullet -}, \quad k = 2.0 \times 10^{12}\ \mathrm{L/(mol\,s)}, \tag{9}$$

$$C_{10}H_8 + H \rightarrow C_{10}H_9^{\bullet}, \quad k = 3.4 \times 10^{9}\ \mathrm{L/(mol\,s)}. \tag{10}$$

Although toluene and naphthalene are difficult to dissolve in water and Triton X-100 is mainly distributed at the interface, they can evidently affect the radiolytic reduction of $CuSO_4$, implying that oil phase is the main source of e_{aq}^-. Therefore, the mechanism of radiolytic reduction of Cu^{2+} in microemulsion should be clarified as follows.

4.1. Effect of the ω value

As mentioned in the introduction, the yield of e_{aq}^- usually increases when the ω value increases. Thus, it is not difficult to understand that the reduction product of $Cu(NO_3)_2$ can be transformed from Cu_2O to Cu when the ω value is increased in the Brij 30 system (Table 1).

4.2. Effect of anion

Table 2 shows the reactions between e_{aq}^- and different anions used in this work and the corresponding rate constants. It can be found that the rate constant of the reaction between e_{aq}^- and NO_3^- is much higher than those of other reactions. In other

Table 2
Rate constants for the reactions between e^-_{aq} and different anions [39]

Anion	Reaction	Rate constant (L/(mol s))
NO_3^-	$NO_3^- + e^-_{aq} \rightarrow NO_3^{2-}$	9.7×10^9
SO_4^{2-}	$SO_4^{2-} + e^-_{aq} \rightarrow$ products	$<1.0\times10^6$
Cl^-	$Cl^- + e^-_{aq} \rightarrow$ products	$<1.0\times10^6$

words, NO_3^- can scavenge e^-_{aq} and decrease its yield effectively, while the ability of SO_4^{2-} and Cl^- is much weaker. Although the rate constant of the reaction between e^-_{aq} and Br^- is short, it can be supposed that the ability of Br^- and Cl^- to scavenge e^-_{aq} is similar because of their similar nature. Thus, in the Brij 56 system, it is easy to understand that the reduction product of $Cu(NO_3)_2$ is Cu_2O, while the reduction products of $CuSO_4$, $CuCl_2$, and $CuBr_2$ are Cu.

In the Triton X-100 system, the reduction products of $CuCl_2$ and $CuBr_2$ are different from that of $CuSO_4$, which is not similar to the phenomenon in the Brij 56 system (Table 1). There may be a different mechanism of reduction. Kapoor et al. [42] have studied the influence of I^- on the formation and stabilization of Cu nanoparticles and considered that I^- can stabilize the Cu^+ intermediate and the final Cu nanoparticles. They also found that Cl^- and Br^- have similar behavior [42]. Here, it may be the X^- (X = Cl, Br) that prevents the hydrolysis of Cu^+ and the generation of Cu_2O. Thus, although the rate constant of the reaction of e^-_{aq} with SO_4^{2-} is close to those of e^-_{aq} with Cl^- and Br^-, the reduction product of $CuSO_4$ is Cu_2O, while those of $CuCl_2$ and $CuBr_2$ are Cu in the Triton X-100 system (Table 1).

Besides the effect on the chemical composition, the anion can also affect the morphology of the reduction product of Cu^{2+}. In the Brij 30 system, the morphologies of the radiolytic reduction products of Cu^{2+} are different (Figs. 2C–2F). The aspect ratio of rodlike Cu nanoparticles obtained from $Cu(NO_3)_2$ is obviously higher than those obtained from $CuSO_4$ and $CuCl_2$, and rodlike Cu nanoparticles seldom appear when $CuBr_2$ is used as precursor. This does not accord with the Hofmeister series of anions, $SO_4^{2-} > Cl^- > Br^- > NO_3^-$ [34], which was suggested to occur in the effect of anions on the morphology of $Mg(OH)_2$ nanoparticles [43]. Moreover, our result does not agree with the result of Pileni and co-workers [34], either. It was found that Cl^- favored the generation of Cu nanorods with higher aspect ratio in the $Cu(AOT)_2$–isooctane–water system, where hydrazine was used as a reducing agent [34]. This phenomenon was ascribed to the preferential adsorption of Cl^- on the (001) faces and the faster growth on the (111) faces of Cu nanocrystals [34]. However, NO_3^- did not exhibit a similar action [34]. Considering the different situation from that in the literature, we suggest here that the unique phenomenon of NO_3^- in this study can be attributed to its strong effect on the yield of e^-_{aq}. In detail, NO_3^- can greatly decrease the yield of e^-_{aq} and thus the rate of reduction to such an extent that the difference of the growth rates between different crystal faces is large enough to form Cu nanorods. In other word, the morphology of nanoparticles may be controlled by the yield of e^-_{aq}. An interesting work will be reported in a forthcoming article, where solid and hollow Cu_2O nanocubes are synthesized via controlling the yield of e^-_{aq}.

4.3. Effect of the aromatic ring

As the above illustrates, e^-_{aq} can be mainly generated from the scavenging of e^-_{oil} by water pool [22–25]. If e^-_{oil} is scavenged by some groups during its migration into the water pool, i.e., the aromatic ring in toluene, naphthalene, or Triton X-100, the concentration of e^-_{aq} in water pool will decrease. This does not favor the further reduction of Cu^+ (Eq. (5)) and is therefore propitious for the formation of Cu_2O. So the reduction product of $CuSO_4$ in the Brij 56 system is Cu, while it is Cu_2O in the Triton X-100 system. When toluene or naphthalene is added to the Brij 56 system, the reduction product of $CuSO_4$ can be transformed from Cu to Cu_2O.

4.4. Effect of the length of polyoxyethylene chain in surfactant

Celik and Dag [44] have shown that the polyoxyethylene chain of $C_{12}H_{25}(OCH_2CH_2)_{10}OH$ can form hydrogen bonds with transition metal aqua complexes. Here, the polyoxyethylene chain in Brij 56 is longer than that in Brij 30. Thus, Brij 56 may efficiently coordinate with Cu^{2+} and Cu^+ and decrease their oxidation–reduction potential, which will not favor the reducing reaction, while the effect of Brij 30 on the oxidation–reduction potential may be weaker. This may be used to explain the different reduction products of $Cu(NO_3)_2$ in the Brij 56 and Brij 30 systems (Table 1).

5. Conclusions

In nonionic surfactant (Brij 30, Brij 56, and Triton X-100)-based microemulsions, the ω value, anion, and surfactant can remarkably affect the radiolytic reduction of Cu^{2+} and the morphologies of the reduction products simultaneously. With increasing ω value, the yield of e^-_{aq} is increased and leads to the transformation of the reduction product of $Cu(NO_3)_2$ from Cu_2O to Cu. Because the aromatic ring can scavenge e^-_{oil} and decrease the yield of e^-_{aq}, Triton X-100, the surfactant-containing aromatic ring, favors the generation of Cu_2O. Among the anions studied in this work, NO_3^- can greatly decrease the yield of e^-_{aq}, resulting in the generation of Cu_2O in the Brij 56 system. In addition, NO_3^- may reduce the yield of e^-_{aq} and thus the rate of reduction to such an extent that the difference of the growth rates between different crystal faces is great enough to form Cu nanorod in Brij 30 system. Therefore, it can be concluded that the effects of the ω value, the anion, and the structure of the surfactant on the yield of e^-_{aq} play a key role in the radiolytic reduction of Cu^{2+}. It is also suggested that the morphology of reduction product may be controlled by the yield of e^-_{aq}. The above results demonstrate that the combination of γ-irradiation and W/O microemulsion can afford us more unique conditions to control the synthesis of nanoparticles than the routine chemical method in microemulsion. For the first time, the compounds with aromatic ring have

been used to control the synthesis of nanoparticles, which is impossible in routine chemical methods. Moreover, anions, especially NO_3^-, may affect the composition and morphology of nanoparticles via their effect on the yield of e_{aq}^-, which is remarkably different from the mechanism in routine chemical method. It is believed that the results reported herein will make the synthesis of nanoparticles in microemulsion more abundant. At the same time, our results further confirm the validation of the mechanism concerning the producing of e_{aq}^- in microemulsion and indicate its wide application in the controlled synthesis of nanoparticles. The generation, migration, and quenching of electrons can also afford us some structural information on microemulsions.

Acknowledgments

This work was supported by the Natural Science Foundation of China (Grants 90206020, 29901001). Sincere thanks are due to Xiuzheng Gai and Yuping Wang in the Electron Microscopy Laboratory, Peking University, and Ping He in our group for help with TEM experiments and to Deliang Sun for assistance in the γ-irradiation experiments.

Supporting information

The online version of this article contains additional supporting information.

Please visit DOI:10.1016/j.jcis.2006.12.021.

References

[1] C. Burda, X.B. Chen, R. Narayanan, M.A. El-Sayed, Chem. Rev. 105 (2005) 1025.
[2] A. Roucoux, J. Schulz, H. Patin, Chem. Rev. 102 (2002) 3757.
[3] A.P. Alivisatos, Science 271 (1996) 933.
[4] Y.G. Sun, Y.N. Xia, Science 298 (2002) 2176.
[5] V. Pillai, P. Kumar, M.J. Hou, P. Ayyub, D.O. Shah, Adv. Colloid Interface Sci. 55 (1995) 241.
[6] J. Eastoe, B. Warne, Curr. Opin. Colloid Interface Sci. 1 (1996) 800.
[7] L.M. Qi, J.M. Ma, H.M. Cheng, Z.G. Zhao, J. Phys. Chem. B 101 (1997) 3460.
[8] M.P. Pileni, in: J.H. Fendler (Ed.), Nanoparticles and Nanostructured Films: Preparation, Characterization and Applications, Wiley–VCH, Weinheim, 1998, p. 71.
[9] L.M. Qi, J.M. Ma, H.M. Cheng, Z.G. Zhao, Colloids Surf. A 108 (1996) 117.
[10] J.D. Hopwood, S. Mann, Chem. Mater. 9 (1997) 1819.
[11] R.P. Bagwe, K.C. Khilar, Langmuir 13 (1997) 6432.
[12] S. Modes, P. Lianos, J. Phys. Chem. 93 (1989) 5854.
[13] A. Henglein, J. Phys. Chem. 97 (1993) 5457.
[14] J. Belloni, M. Mostafavi, H. Remita, J.L. Marignier, M.O. Delcourt, New J. Chem. 22 (1998) 1239.
[15] E.M. Egorova, A.A. Revina, Colloid J. 64 (2002) 301.
[16] S. Kapoor, R. Joshi, T. Mukherjee, Chem. Phys. Lett. 396 (2004) 415.
[17] S. Kapoor, R. Joshi, T. Mukherjee, J.P. Mittal, Res. Chem. Intermed. 27 (2001) 747.
[18] H.K. Wu, X.L. Xu, X.W. Ge, Z.C. Zhang, Radiat. Phys. Chem. 50 (1997) 585.
[19] S. Kapoor, S. Adhikari, C. Gopinathan, J.P. Mittal, Mater. Res. Bull. 34 (1999) 1333.
[20] C.Q. Xu, Y.H. Ni, Z.C. Zhang, X.W. Ge, Q. Ye, Mater. Lett. 57 (2003) 3070.
[21] C.Q. Xu, Z.C. Zhang, H.L. Wang, Q. Ye, Mater. Sci. Eng. B 104 (2003) 5.
[22] P. He, X.H. Shen, H.C. Gao, Acta Phys. Chim. Sin. 20 (2004) 1200.
[23] P. He, X.H. Shen, H.C. Gao, J. Colloid Interface Sci. 284 (2005) 510.
[24] L.M. Qi, J.M. Ma, J.L. Shen, J. Colloid Interface Sci. 186 (1997) 498.
[25] M. Wong, M. Gratzel, J.K. Thomas, Chem. Phys. Lett. 30 (1975) 329.
[26] J.L. Gebicki, L. Gebicka, J. Kroh, J. Chem. Soc. Faraday Trans. 90 (1994) 3411.
[27] S. Adhikari, R. Joshi, C. Gopinathan, J. Colloid Interface Sci. 191 (1997) 268.
[28] R. Joshi, T. Mukherjee, Radiat. Phys. Chem. 66 (2003) 397.
[29] M.P. Pileni, B. Hickel, C. Ferradini, J. Pucheault, Chem. Phys. Lett. 92 (1982) 308.
[30] M.P. Pileni, P. Brochette, B. Hickel, B. Lerebours, J. Colloid Interface Sci. 98 (1984) 549.
[31] Y. Zhao, J.J. Zhu, J.M. Hong, N.S. Bian, H.Y. Chen, Eur. J. Inorg. Chem. (2004) 4072.
[32] C. Salzemann, I. Lisiecki, A. Brioude, J. Urban, M.P. Pileni, J. Phys. Chem. B 108 (2004) 13242.
[33] H.R. Zhang, C.M. Shen, S.T. Chen, Z.C. Xu, F.S. Liu, J.Q. Li, H.J. Gao, Nanotechnology 16 (2005) 267.
[34] A. Filankembo, S. Giorgio, L. Lisiecki, M.P. Pileni, J. Phys. Chem. B 107 (2003) 7492.
[35] S. Banerjee, D. Chakravorty, Europhys. Lett. 52 (2000) 468.
[36] Y.J. Xiong, Z.Q. Li, R. Zhang, Y. Xie, J. Yang, C.Z. Wu, J. Phys. Chem. B 107 (2003) 3697.
[37] Y.H. Lee, I.C. Leu, S.T. Chang, C.L. Liao, K.Z. Fung, Electrochim. Acta 50 (2004) 553.
[38] V.I. Tupikov, in: V.K. Milinchuk, V.I. Tupikov (Eds.), Organic Radiation Chemistry Handbook, Ellis Horwood Limited, Chichester, 1989, p. 44.
[39] G.V. Buxton, C.L. Greenstock, W.P. Helman, A.B. Ross, J. Phys. Chem. Ref. Data 17 (1988) 513.
[40] Because the rate constants of relative solutes with H in cyclohexane are short, there only list the relative data in other solvent for reference. If the solvent is not marked, water is used.
[41] Y.J. Zhu, Y.T. Qian, M.W. Zhang, Z.Y. Chen, D.F. Xu, L. Yang, G. Zhou, Mater. Res. Bull. 29 (1994) 377.
[42] S. Kapoor, R. Joshi, T. Mukherjee, Chem. Phys. Lett. 354 (2002) 443.
[43] R. Giorgi, C. Bozzi, L. Dei, C. Gabbiani, B.W. Ninham, P. Baglioni, Langmuir 21 (2005) 8495.
[44] O. Celik, O. Dag, Angew. Chem. Int. Ed. 40 (2001) 3799.